Note that if the content of a second component of any binary alloy is significant, ternary and two kinds of binary compounds are likely to form in the alloy-boron transition zone, either as a one-phase or multi-phase layers. Effect of the second component on the properties of boride coatings will be illustrated using the Fe–Cr–B system as an example.

As evidenced from its isothermal section at 900ºC [37], iron, chromium and boron do not form any ternary compound, while seven compounds CrB_4, CrB_2, Cr_2B_3, Cr_3B_4, CrB, Cr_5B_3 and Cr_2B are known to exist in the Cr–B binary system. Therefore, formation of a complicated structure of boride coatings on the surface of solid samples of Fe–Cr alloys and high chromium steels during their thermochemical boriding may be expected.

Experimental data [38-49] on the interaction of five iron-chromium alloys (5–30% Cr) and two industrial steels containing 13 and 25% chromium with boron in a mixture of amorphous boron powder and KBF_4 (activator) in the temperature range of 850–950ºC at reaction times up to 43200 s are juxtaposed and discussed together with findings of other researchers in this work.

First, attention is paid to the phase identification of boride layers formed at the interface of a solid Fe–Cr alloy or steel with boron and the determination of their chemical composition. Two types of layer microstructure (one-phase and two-phase) are shown to occur, depending upon the chromium content of an alloy or steel.

Then, mechanism of layer formation is considered in detail from a chemical viewpoint to provide evidence for the inadequacy of some too simplified diffusional imaginations existing in the available literature.

Also, a system of differential equations describing layer-growth kinetics and taking account of both the rate of counter-diffusion of iron and boron atoms across layer bulks and the rate of subsequent chemical transformations at phase interfaces is analyzed to show why in many cases the solid-state growth of boride or any other compound layers is neither simultaneous, nor parabolic.

Eventually, interconnection between the structure and mechanical properties, notably the dry abrasive wear resistance and the microhardness of boride layers formed on the surface of alloy and steel samples, is demonstrated.

2. EXPERIMENTAL PROCEDURE

2.1. Materials and Samples

The materials used for the preparation of iron-chromium alloys included carbonyl iron powder (99.98% Fe) and electrolytic-grade chromium platelets (99.98% Cr). All contents are given in mass percent if otherwise not stated. Reagents were amorphous boron powder (98.3% B) and analytical-grade KBF_4.

Cylindrical rods of Fe–Cr alloys (5, 10, 15, 25 and 30% chromium) were prepared by arc-melting of appropriate amounts of metals under argon, with subsequent casting the melts into water-cooled copper crucibles. The rods were annealed at 1100ºC for 2 h to ensure their homogenization.

Rods (16 mm diameter) of industrial steels were used in the as-received condition (without any additional heat treatment). The content of main components of a 13% Cr steel was 85.2% Fe, 13.6% Cr, 0.38% C, 0.30% Mn, 0.30% Si and 0.20% Ni. 25% Cr steel contained 72.8% Fe, 25.2% Cr, 0.13% C, 0.50% Mn, 0.46% Si, 0.45% Ni and 0.28% Ti. The microstructure of Fe–Cr alloys consisted of the body centered cubic -phase (ferrite), while that of the steels also contained fine inclusions of iron and chromium carbides.

Specimens in the form of tablets, 11.28 mm in diameter (1.0 cm^2 area) and 5.5 mm high, were machined from the Fe–Cr alloy and steel rods. Flat sides of the tablets were ground and polished mechanically.

2.2. Experimental Methods

The vacuum device employed for boriding solid samples, details of the boriding procedure and investigational techniques used to characterize initial samples and boride layers formed on their surface have been described elsewhere [36,47-49].

The alloy or steel tablet was embedded into a mixture of boron powder and 5% KBF_4 as an activator. KBF_4 is considered to be one of most effective activators due to the formation of volatile compounds, mainly BF_3, at elevated temperatures [1,2]. Compared to other boriding agents such as $Na_2B_4O_7$, a mixture of 70% $Na_2B_4O_7$ with 30% SiC or a mixture of 65-70% $Na_2B_4O_7$ with 35-30% B_4C, its application allows much thicker and regular boride layers to be obtained under similar temperature-pressure conditions.

Experiments were carried out at a temperature of 850, 900 and 950ºC under high-purity argon (99.999 vol.% Ar) at a reduced pressure of 2.5 10^4 Pa. Their duration was 3600–43200 s (1–12 h).

3. RESULTS AND DISCUSSION

3.1. Types of Microstructure of Boride Layers

3.1.1. Phase Identity and Chemical Composition of Boride Layers

At a temperature of 850, 900 and 950ºC and sufficiently long reaction times, two compact boride layers were found to form on the surface of all alloy and steel samples investigated. The constituent phases of the layers were identified by plan-view layer-by-layer X-ray diffraction analysis. Two types of their microstructure (one-phase and two-phase) were revealed, as exemplified in Figures (**1** and **2**).

Comparison of angles 2 and spacing *d* of experimental X-ray patterns obtained with the literature data for iron and chromium borides [50-55] indicated that in the case of 5–15% Cr alloys and a 13% Cr steel the outer boride layer bordering the boriding agent is a solid solution based on the FeB chemical compound,

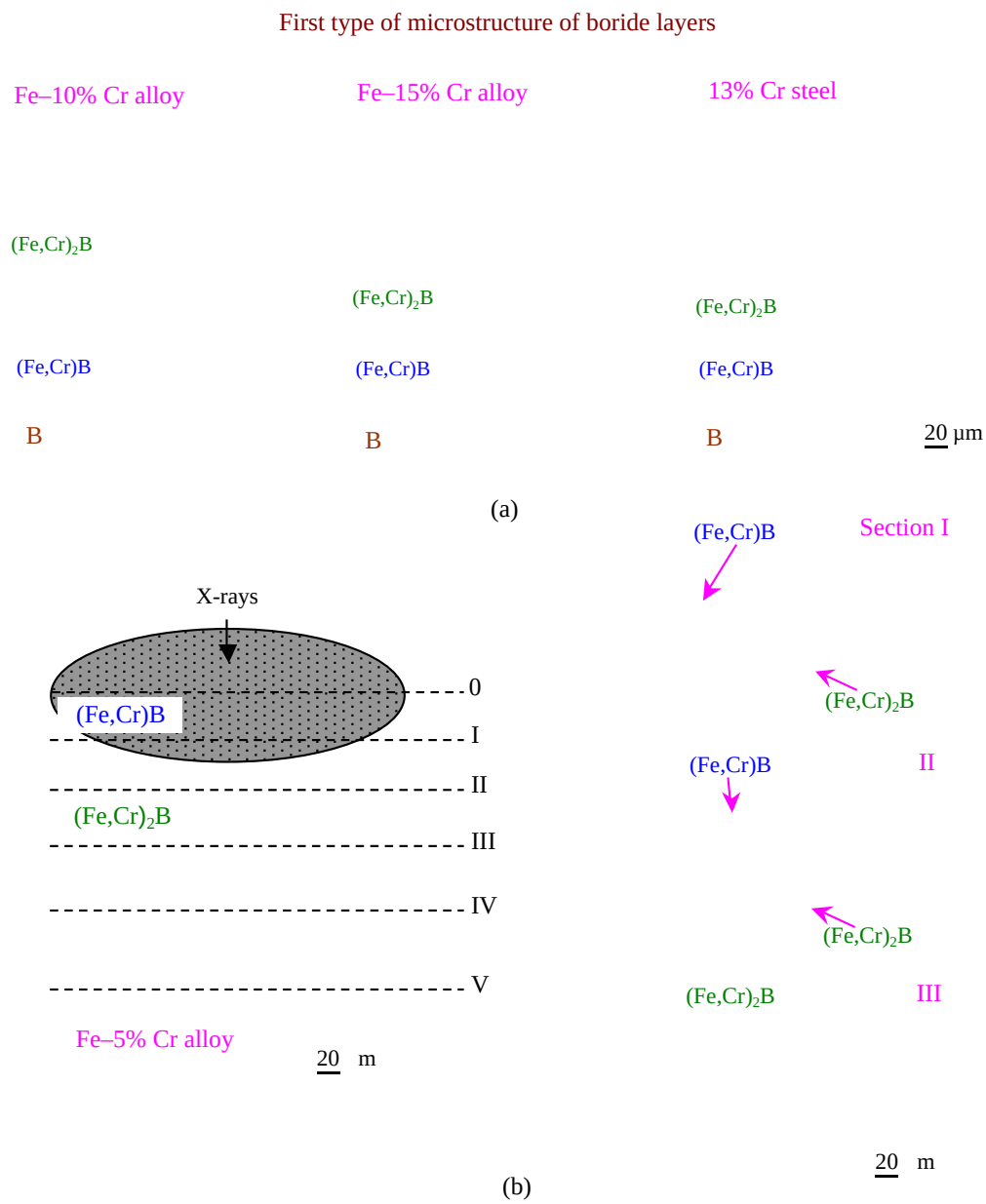

Figure 1: (a) Microstructure of the transition zone of borided Fe–10% Cr alloy, Fe–15% Cr alloy and 13% Cr steel samples. **(b)** Scheme of X-ray diffraction investigations of borided Fe–5% Cr alloy samples and the microstructure of appropriate layer sections. Boriding conditions: temperature 950°C, reaction time 21600 s.

Figure 2: (a) Microstructure of the transition zone of borided Fe–25% Cr alloy, Fe–30% Cr alloy and 25% Cr steel samples. **(b)** Scheme of X-ray diffraction investigations of borided Fe–25% Cr samples and the microstructure of appropriate layer sections. Boriding conditions: temperature 950°C, reaction time 21600 s.

while the inner boride layer adjacent to the solid substrate is a solid solution based on the Fe_2B chemical compound. Each of two layers is one-phase. Their chemical compositions are provided in Table **1** for a Fe–5% Cr alloy as an example [48,49]. It is the first type of their microstructure, which is usually observed with steels [1-7,13-31]. Chromium content of the layers is rather significant. Its values vary in the range 3-12 at.%.

Even though the microstructure of boride layers on Fe–25% Cr alloy, Fe–30% Cr alloy and 25% Cr steel samples is readily seen in Figure **2** to be two-phase, their X-ray patterns were identical to those of 5–15% Cr alloy and 13% Cr steel ones and corresponded to the FeB chemical compound for the outer layer and the Fe_2B chemical compound for the inner layer (Figure **3**). In view of the relatively high chromium content of Fe–25% Cr and Fe–30% Cr alloys and a 25% Cr steel, of

Table 1: Iron, Chromium and Boron Contents of Reacting Phases, Found by EPMA Measurements on Borided Fe–5% Cr Alloy Samples after their X-Ray Diffraction Investigations, See also Figure 1

Section in Figure 1b	Region	Content (mass%/at.%)			Phase
		Fe	Cr	B	
0	One-phase	79.5/47.3	4.2/2.7	16.3/50.0	(Fe,Cr)B
I	Darker in Section I of Figure **1b**	80.0/48.1	4.1/2.6	15.9/49.3	(Fe,Cr)B
	Brighter in Section I of Figure **1b**	86.1/62.3	4.8/3.8	9.1/33.9	$(Fe,Cr)_2B$
II	Darker in Section II of Figure **1b**	79.0/46.5	4.3/2.7	16.7/50.8	(Fe,Cr)B
	Brighter in Section II of Figure **1b**	87.0/63.7	4.4/3.4	8.7/32.8	$(Fe,Cr)_2B$
III	One-phase (Section III of Figure **1b**)	86.6/63.1	4.5/3.5	8.9/33.4	$(Fe,Cr)_2B$
IV	Darker	87.1/63.7	4.2/3.3	8.7/33.0	$(Fe,Cr)_2B$
	Brighter	95.1/94.8	4.9/5.2	0.0/0.0	<Fe>
V	One-phase	95.0/94.6	5.0/5.4	0.0/0.0	<Fe>

2 (deg)

Figure 3: X-ray diffraction patterns of the outer and inner boride layers formed on **(a)** 13% Cr steel and **(b)** Fe–25% Cr alloy samples. Appropriate pairs of the patterns are seen to be similar, excepting the reflection intensities. Boriding conditions: 950°C, 21600 s.

Table 2: Iron, Chromium and Boron Contents of Reacting Phases, Found by EPMA Measurements on Borided Fe–25% Cr Alloy Samples after their X-Ray Diffraction Investigations, See also Figure 2

Section in Figure 2b	Region	Content (at.%)			Phase
		Fe	Cr	B	
I	Brighter in Figure **2b**	25.9 29.0 26.9 29.2 33.1	23.9 22.9 21.1 19.9 16.2	50.2 48.1 52.0 50.9 50.7	(Fe,Cr)B
	Darker in Figure **2b**	23.7 22.0 17.7 20.9 15.0	24.4 29.5 32.2 29.8 33.1	51.9 48.5 50.1 49.2 51.9	(Cr,Fe)B
III	**A** in Figure **2b**	56.6 53.9 50.0	12.2 11.5 16.2	31.2 34.6 33.8	$(Fe,Cr)_2B$
	B in Figure **2b**	18.4 24.2 19.6	46.8 44.1 46.8	34.8 31.7 33.6	$(Cr,Fe)_2B$
	C in Figure **2b**	79.4 77.5 81.9	20.6 22.5 18.1	0.0 0.0 0.0	<Fe>
IV	Brighter in Figure **2b**	76.1 80.1 74.2	23.9 19.4 25.8	0.0 0.5 0.0	<Fe>
	Darker in Figure **2b**	18.8 19.0 19.6	49.2 47.0 50.7	32.1 34.0 29.7	$(Cr,Fe)_2B$
V	Brighter	72.8 72.2 72.5	27.2 27.8 27.5	0.0 0.0 0.0	<Fe>
	Darker	23.4 18.6 21.8	43.1 48.7 45.1	33.5 32.7 33.1	$(Cr,Fe)_2B$
VI	One-phase	73.9 73.0 73.7	26.1 27.0 26.3	0.0 0.0 0.0	<Fe>

seven known compounds CrB_4, CrB_2, Cr_2B_3, Cr_3B_4, CrB, Cr_5B_3 and Cr_2B [37], the formation of at least CrB and Cr_2B phases could be expected. This is indeed the case, though X-ray diffraction analysis does not show the presence of any chromium boride in the transition zone between the reactants. Each of two boride layers is two-phase and consists of distinct darker and brighter regions differing by their chemical composition. It is the second type of microstructure of boride layers, which has been overlooked by previous researchers, most probably for the following two reasons.

(1) Presence of the CrB and Cr_2B compounds is not revealed by X-ray diffraction or any other method of structural analysis.

(2) This type of microstructure is much less profound with alloys and steels of complicated chemical composition than with binary Fe–Cr alloys due to the strong influence of other constituting elements of solid substrates (C, P, S, Si, Mn, Ni, Ti, Mo, W and others). Therefore, previous researchers dealing with steels have not noticed this unexpected two-phase microstructure.

EPMA measurements clearly indicate that iron prevails in brighter regions, while chromium is dominant in darker ones of any boride layer. An example is presented in Table **2** for a Fe–25% Cr alloy [49].

Thus, the outer boride layer consists of a mixture of crystals of the (Fe,Cr)B and (Cr,Fe)B phases. Nonetheless, even most strong reflections of CrB (spacing, d = 0.2350, 0.1965 and 0.1255 nm) and Cr_2B (d = 0.2590, 0.2158 and 0.2043 nm) [54,55] were missing from experimental X-ray patterns of boride layers formed in

Fe–25% Cr and Fe–30% Cr alloy and 25% Cr steel samples. With Fe–25% Cr and Fe–30% Cr alloys, microstructure of both layers has a distinguishable regular arrangement, which is hardly observable in 25% Cr steel samples (compare the microstructure of Section I of Figure **2** with that of Section II of Figure **4**).

Shown in Figure **4** are micrographs of longitudinal and plan-view sections for a 25% Cr steel. Sections 0-II of borided steel samples corresponds to the outer boride layer. These clearly show how the two-phase microstructure is formed. First, the homogeneous (Fe,Cr)B phase appears to occur. Then, regions of different chromium content are developed within its bulk, as seen in Section I where major phase is (Fe,Cr)B of different chemical composition. The chromium content of its brighter regions is 7-12 at.%, while that of the darker ones is up to 20 at.% (Table **3**).

Figure 4: Scheme of X-ray diffraction investigations of borided Fe–25% Cr steel samples and the microstructure of appropriate layer sections. Boriding conditions: temperature 950°C, reaction time 21600 s.

Table 3: Average Iron, Chromium and Boron Contents of Reacting Phases, Found by EPMA Measurements on Borided 25% Cr Steel Samples after their X-Ray Diffraction Investigations, See also Figure 4

Section in Figure 4	Region	Content (mass %/at.%)			Phase
		Fe	Cr	B	
I	Brighter in Section I of Figure **4**	71.4/42.2	12.2/7.7	16.4/50.1	(Fe,Cr)B
	Darker in Section I of Figure **4**	53.8/31.8	30.2/19.1	16.1/49.1	(Fe,Cr)B
II	Brighter in Section II of Figure **4**	54.3/31.6	28.9/18.1	16.8/50.3	(Fe,Cr)B
	Darker in Section II of Figure **4**	21.9/12.6	61.6/38.2	16.5/49.2	(Cr,Fe)B
III	Brighter in Section III of Figure **4**	68.1/48.6	22.6/17.3	9.3/34.1	$(Fe,Cr)_2B$
	Darker in Section III of Figure **4**	24.6/17.4	66.8/51.0	8.6/31.6	$(Cr,Fe)_2B$
IV	Brighter in Section IV of Figure **4**	84.1/83.2	15.9/16.8	0.0/0.0	<Fe>
	Darker in Section IV of Figure **4**	27.0/18.8	63.8/48.0	9.2/33.2	$(Cr,Fe)_2B$
V	Brighter in Section V of Figure **4**	81.3/80.2	18.7/19.8	0.0/0.0	<Fe>
	Darker in Section V of Figure **4**	24.6/17.4	66.8/51.0	8.6/31.6	$(Cr,Fe)_2B$
VI	Homogeneous	80.7/79.6	19.3/20.4	0.0/0.0	<Fe>

It is the beginning of formation of the two-phase microstructure of the outer boride layer. Fine black spots in this section are probably iron and chromium carbides and borocarbides, while large black spots are holes. A mixture of crystals of the (Fe,Cr)B and (Cr,Fe)B phases are present in Section II. It is the fully developed microstructure of the second type.

Section III crosses the inner boride layer. Its microstructure is seen to be two-phase. The brighter phase is $(Fe,Cr)_2B$, while the darker phase is $(Cr,Fe)_2B$.

Section IV corresponds to a solid solution of chromium in iron <Fe> and the $(Cr,Fe)_2B$ phase. The microstructure of section V is similar to that of section IV, with the amount of the $(Cr,Fe)_2B$ phase being much less. Section VI is the steel base, somewhat depleted in chromium. Section VII is entirely the steel base of nominal composition. Thus, the reaction zone extends to around 200 m from this section to the top of a boride coating.

It can be concluded that the presence of the (Cr,Fe)B phase in boride layers is not revealed by XRD or other methods of structural analysis because under highly non-equilibrium conditions the lattice rearrangement FeB " CrB is not completed in view of time limitations. Therefore, part of iron sites of the FeB lattice, very similar to that of the CrB one, is merely replaced by chromium atoms, without any noticeable structural changes.

In other words, the non-equilibrium CrB phase crystallizes in the FeB lattice. Hence, being far from equilibrium, the outher boride layer appears to be single-phase structurally (crystallographically) and two-phase compositionally (chemically) [49].

Similar considerations are clearly applicable to another pair of phases Fe_2B and Cr_2B, which are the constituents of the inner boride layer. Therefore, formation of the (Cr,Fe)B and $(Cr,Fe)_2B$ phases, readily seen visually in the microstructure of boride layers occurred on the surface of borided Fe–25% Cr alloy, Fe–30% Cr alloy and 25% Cr steel samples and additionally verified by EPMA measurements, can hardly be doubted.

As long as both boride layers are two-phase, distribution of chromium within their bulks is found to be very irregular (Figure **5**). Wherever the chromium content increases, the iron content decreases, and vice versa. In any sufficiently large area, however, chemical composition of each of two layers coincides with the stoichiometry of an appropriate compound, as it should be from a chemical viewpoint.

It is worth noting that some evidence for a change of the first-to-second type of microstructure of boride layers may already be noticed with Fe–15% Cr alloy samples. As seen in Figure **6**, in this case the microstructure of the transition zone between the reactants is somewhat different from that with Fe–5% Cr and Fe–10% Cr alloys. Sections 0 and I of a borided Fe–15% Cr sample corresponds to the (Fe,Cr)B phase. Sections II and III cross both the (Fe,Cr)B and $(Fe,Cr)_2B$ phases, with the (Fe,Cr)B phase dominating in Section II and $(Fe,Cr)_2B$ phase prevailing in Section III. Section IV corresponds to the single $(Fe,Cr)_2B$ phase. Microstructure of Sections V and VI consists mostly of the alloy base of somewhat changed composition compared to the nominal one with inclusions of crystals of the $(Fe,Cr)_2B$ and occasionally (Cr, Fe)$_2$B phase. Section VII is entirely the alloy base Fe–Cr of nominal composition 85% Fe–15% Cr. Chemical composition of

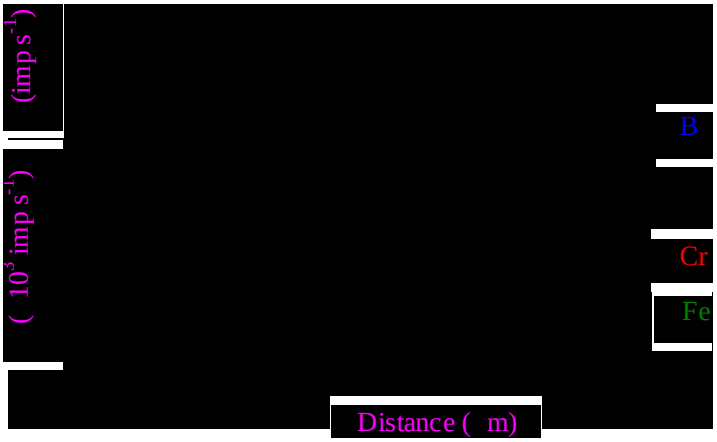

Figure 5: Concentration profiles of boron, iron and chromium in the 25% Cr steel-boron transition zone. Boriding conditions: temperature 950ºC, reaction time 21600 s.

Figure 6: Scheme of X-ray diffraction investigations of borided Fe–15% Cr alloy samples and the microstructure of appropriate layer sections. Boriding conditions: temperature 950ºC, reaction time 21600 s.

Table 4: Iron, Chromium and Boron Contents of Reacting Phases, Found by EPMA Measurements on Borided Fe–15% Cr Alloy Samples after their X-Ray Diffraction Investigations, See also Figure 6

Section in Figure 6	Region	Content (mass%/at.%)			Phase
		Fe	Cr	B	
I	One-phase	71.7/42.6	12.1/7.7	16.2/49.7	(Fe,Cr)B
II	Darker in Section II of Figure **6**	70.7/41.7	12.8/8.1	16.5/50.2	(Fe,Cr)B
	Brighter in Section II of Figure **6**	77.8/56.4	13.3/10.3	8.9/33.3	$(Fe,Cr)_2B$
IV	One-phase	76.9/55.9	14.3/11.1	8.8/33.0	$(Fe,Cr)_2B$
V	**A** in Section V of Figure **6**	78.8/57.9	12.8/10.1	8.4/32.0	$(Fe,Cr)_2B$
	B in Section V of Figure **6**	88.1/87.3	11.9/12.7	0.0/0.0	<Fe>
	C in Section V of Figure **6**	46.9/35.9	44.3/31.6	8.8/32.5	$(Fe,Cr)_2B$
VI	**B** in Section VI of Figure **6**	87.4/85.9	12.4/13.1	0.0/0.0	<Fe>
	C in Section VI of Figure **6**	54.5/38.6	36.3/27.7	9.2/33.7	$(Fe,Cr)_2B$
VII	One-phase	85.2/84.3	14.8/15.7	0.0/0.0	<Fe>

the alloy-boron transition zone in its different sections is presented in Table **4**.

Comparison of micrographs shown in Figure **6** indicates that, in addition to two (Fe,Cr)B and Fe_2B boride layers typical of all three Fe–5% Cr, Fe–10% Cr and Fe–15% Cr alloys, thin long crystals are formed near the Fe_2B layer in the case of a Fe–15% Cr alloy. These are highly enriched in chromium and penetrate deep into the alloy base. Their chemical composition largely corresponds to that of the $(Fe,Cr)_2B$ phase containing up to 45% or 32 at.% chromium. This composition is already close to that of the $(Cr,Fe)_2B$ phase. The width of the area they occupy is comparable with the thickness of boride layers. Like the latter, it increases with passing time.

Probably, with alloys containing more than 15% Cr this area gradually transforms into a two-phase boride layer. To follow this transformation, experiments with binary Fe–Cr alloys of chromium content between 15% and 25%, for example 17.5%, 20% and 22.5%, would be desirable.

3.1.2. Formation of Texture of Boride Layers

Even though the literature and experimental values of angles 2 and spacing *d* were found to agree fairly well, appropriate peak intensities disagreed very considerably with all alloys and steels studied.

For example, in the case of a Fe–15% Cr alloy, strongest reflections were {002} (2 = 63.07^{o} for Cu K! radiation and spacing, *d* = 0.1474 nm) and, to a lesser extent, {020} (2 = 32.63º and *d* = 0.2744 nm) for the orthorhombic FeB phase (outer boride layer), and {002} (2 = 42.55º and *d* = 0.2125 nm) for the tetragonal Fe_2B phase (inner boride layer) [43]. Note that with isotropic microcrystalline samples the strongest reflections are {111} (*d* = 0.21863 nm) {021, 200} (0.20086 nm) and {210} (0.19002 nm) for FeB and {211} (*d* = 0.20126 nm), {310} (0.16159 nm) and {213} (0.12039 nm) for Fe_2B [50-53].

It means that both layers possess a pronounced {002} texture and therefore consist of columnar crystals oriented preferentially in the direction of diffusion. This is considered to be a consequence of the existence of paths of enhanced diffusion in the crystal lattices of FeB and Fe_2B [2]. If such paths are not available (close rates of diffusion in all crystallographic directions), almost flat boride layers are formed. The same happens if these paths are blocked by atoms of additives or impurities.

The change in intensities of most characteristic reflections with increasing distance from the surface of a borided Fe–15% Cr alloy tablet is illustrated in Figure **7** as an example [43,49]. The larger orientation order is always observed for the inner portions of both boride

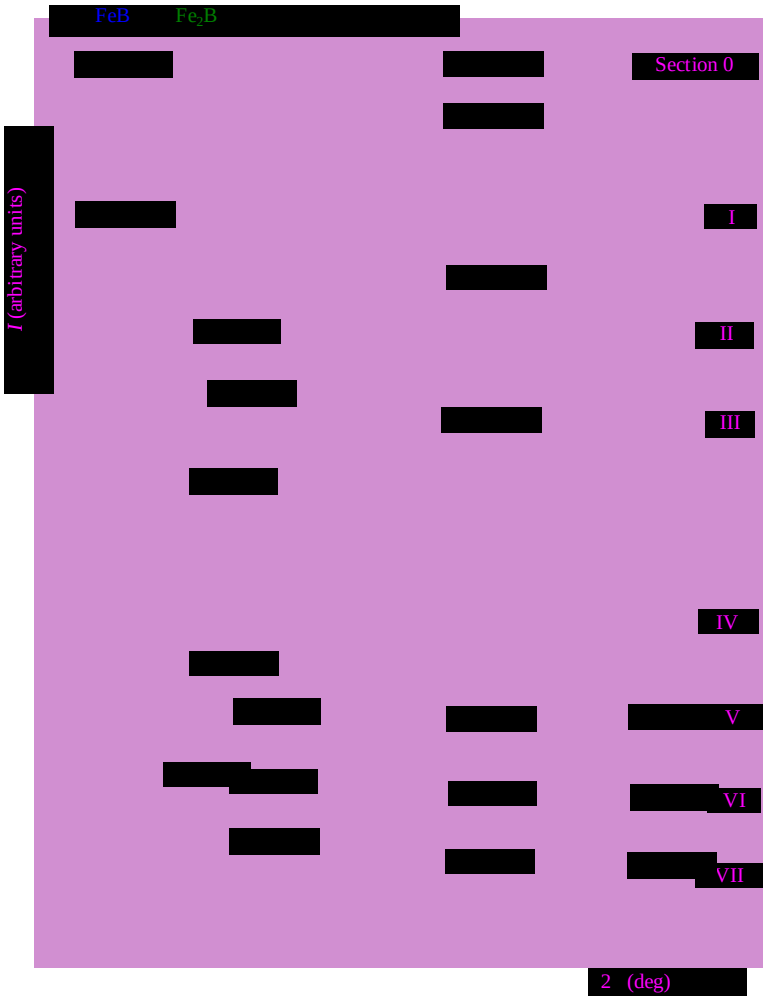

Figure 7: Most intensive reflections of X-ray diffraction patterns taken from different plan-view sections of a Fe–15% Cr alloy sample borided at 950ºC for 21600 s, see also Figure **6**.

layers compared to their near-interface portions. This is easily explainable because near-interface portions of any boride layer, where chemical reactions take place, are less equilibrated compared to its inner portions. Therefore, near-interface crystals have less time to align in the preferred direction. More details about the process of ordering of any boride layer eventually resulting in the formation of its texture, as illustrated in Figure **8**, can be found, for example, in [2,20].

3.2. Mechanism of Formation of Boride Layers

3.2.1. Sequence of Layer Occurrence

Available experimental data show that the formation of boride layers is sequential rather than simultaneous [1,2,46-49]. The Fe_2B layer is the first to form. In the case of a Fe–5% Cr alloy (Figure **9**), this single boride layer was found to grow up to a reaction time of at least 14400 s (4 h) [45-49].

After a reaction time of 3600 s (1 h) at 950 °C, the FeB layer is still missing from the Fe–10% Cr alloy-boron interface, while the Fe_2B layer thickness is already around 70 m. At this temperature, both layers are observed at a reaction time of 7200 s (2 h) or more. In the temperature range of 850–950 °C, a reaction time of 3600 s (1 h) was found to be sufficient for both boride layers to form on the surface of samples of other alloys and steels investigated.

3.2.2. Chemical Reactions at Layer Interfaces

Immediate chemical reaction is possible initially between the surface iron and boron atoms to form the Fe_2B layer: $2Fe_{surf} + B_{surf} = Fe_2B$. The continuous Fe_2B layer separates the reactants from one another. Subsequently, growth of the Fe_2B layer takes place at the expense of counter-diffusion of iron and boron atoms across its bulk and further two partial chemical reactions $2Fe_{dif} + B_{surf} = Fe_2B$ and $B_{dif} + 2Fe_{surf} = Fe_2B$ pro-

Figure 8: Schematic illustration of aligning the Fe_2B crystals, eventually resulting in the formation of texture of the inner boride layer [2,20].

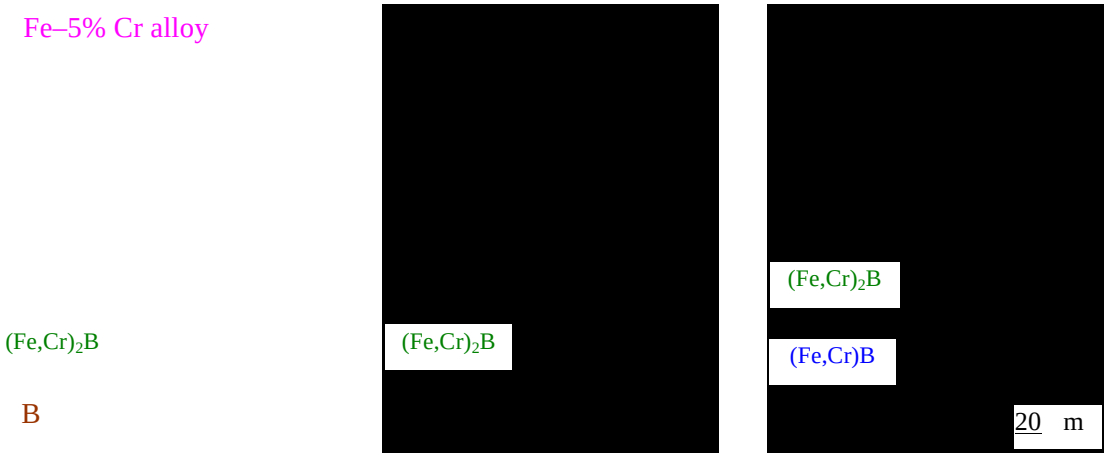

Figure 9: Backscattered electron images (BEI) of the transition zone between a Fe–5% Cr alloy and boron. Boriding conditions: temperature 900ºC, reaction time **(a)** 3600 s, **(b)** 14400 s and **(c)** 21600 s.

ceeding at the B–Fe_2B and Fe_2B–Fe interfaces, respectively.

With passing time, the FeB layer also occurs. It happens when the rate of its consumption in the formation of the first-formed Fe_2B layer proves to be equal to its growth rate.

Under conditions of reaction (chemical) control, when the rate of diffusion of reacting atoms across their bulks exceeds the rate of interfacial (chemical) transformations, growth of the FeB and Fe_2B layers is due to four partial chemical reactions. The FeB layer grows by reactions Fe_{dif} + B_{surf} = FeB at interface 1 and B_{dif} + Fe_2B = 2FeB at interface 2 (Figure **10**). Appropriate increases of its thickness during a time d*t* are dx_{Fe1} and dx_{B2}. The Fe_2B layer grows by reactions Fe_{dif} + FeB = Fe_2B at interface 2 and B_{dif} + $2Fe_{surf}$ = 2FeB at interface 3. Appropriate increases of its thickness during the same time d*t* are dy_{Fe2} and dy_{B3}. Both are consumed at interface 2 in the course of formation of one another. This causes a decrease of their thickness by dx_{-} and dy_{-}, respectively.

It should be emphasized that the arrows of different length and weaker color are intentionally employed in Figure **10** to indicate the decrease in amount of diffusing atoms, available at a particular interface, with increasing distance from a given initial substance (boron or iron). It is obvious that only those boron atoms which have not entered into partial chemical reaction with Fe_2B at interface 2 can diffuse further to interface 3 and enter there into partial chemical reaction with the surface iron atoms. Similarly, only those iron atoms which have not entered into partial chemical reaction with FeB at interface 2 can diffuse further to interface 1 and enter there into partial chemical reaction with the surface boron atoms.

As long as interfacial partial chemical reactions take place at different rates, simultaneous formation of both boride layers can hardly be expected. From a physicochemical viewpoint, their sequential occurrence is more likely, in agreement with experimental observations.

Thickening of the FeB and Fe_2B layers with passing time eventually results in a change of the regime of their growth from reaction controlled to diffusion controlled, when the rate of interfacial transformations (reactions) becomes first equal to, at a certain *critical* layer thickness, and then greater than, at layer thicknesses exceeding this critical value, the rate of diffusion of appropriate reacting atoms to the reaction sites (interfaces) [46-49]. After the FeB layer has reached its critical thickness $x_{critical\ B}$ with regard to boron, the Fe_2B layer loses the source of boron atoms and therefore stops growing at the expense of diffusion of this component.

Similarly, after the Fe_2B layer has reached its critical thickness $y_{critical\ Fe}$ with regard to iron, the FeB layer loses the source of iron atoms and therefore stops growing at the expense of diffusion of this component. Hence, under conditions of diffusion control the FeB and Fe_2B layers are able to grow only at their common interface 2, as shown in Figure **11**. The FeB layer grows at the expense of diffusion of boron atoms across its bulk and their subsequent reaction with the Fe_2B compound. The Fe_2B layer grows at the expense of diffusion of iron atoms across its bulk and their subsequent reaction with the FeB compound.

Figure 10: Schematic diagram illustrating the growth process of the FeB and Fe_2B layers under conditions of reaction (chemical) control. Both layers grow at the expense of diffusion of both components. Arrows of different length and weaker color are employed to indicate the decrease in amount of diffusing atoms, available at a particular interface, with increasing distance from an appropriate initial substance (B or Fe).

Figure 11: Schematic diagram illustrating the growth process of the FeB and Fe_2B layers under conditions of diffusion control. Both layers thicken only at their common interface 2. No partial chemical reactions can take place at interfaces 1 and 3 due to the lack of appropriate diffusing atoms (Fe at interface 1 and B at interface 3).

Both layers are often considered to grow at the expense of diffusion of the single component boron across their bulks. From a physicochemical viewpoint, it is impossible with compact layers having no macroscopic defects and therefore growing by the volume-diffusion mechanism. This assumption is misleading. Moreover, it lacks any experimental support.

Also, compound layers are assumed to grow at the expense of their homogeneity ranges (see, for example, [56,57]. It is another misleading assumption In fact, any compound layer grows at the expense of its stoichiometry. It does not matter, whether a given compound has any range of homogeneity or not. Moreover, the effect of a homogeneity range on compound layer-growth rate is negative and not positive, namely, the greater the homogeneity range, the less is the layer-growth rate [32-34,49].

Note that iron borides FeB and Fe_2B have not got any noticeable homogeneity ranges. Hence, from a diffusional viewpoint their layers should not form at all between iron and boron, in obvious disagreement with available experimental data. It applies not only to metal borides but also to other compounds of whatever chemical nature (oxides, silicides, nitrides, carbides, *etc*.). Any calculations based on this misleading assumption give physically meaningless diffusion coefficients of the components of any chemical compound across its solid layer. This inconsistency is readily overcome in the framework of a physicochemical approach [32-34].

3.3. Layer-Growth Kinetics

Growth kinetics of chemical compound layers are largely treated by using a parabolic relation of the type $x^2 = 2k_1t$, where x is the layer thickness, k_1 is the layer growth-rate constant, and t is the time. It follows from diffusional considerations based on Fick's laws.

With sufficiently thick layers in the micrometer range, parabolic equations are known to produce a satisfactory fit to the experimental data, with iron borides in particular. Note, however, that a more adequate description of growth kinetics of the FeB and Fe_2B layers is provided by a system of two differential equations [32-34,49]

$$\frac{\mathrm{d}x}{\mathrm{d}t} = \frac{k_{0\mathrm{Fe1}}}{1+\dfrac{k_{0\mathrm{Fe1}}x}{k_{1\mathrm{Fe1}}}} + \frac{k_{0\mathrm{B2}}}{1+\dfrac{k_{0\mathrm{B2}}x}{k_{1\mathrm{B2}}}} \quad \frac{rg}{p} \quad \frac{k_{0\mathrm{Fe2}}}{1+\dfrac{k_{0\mathrm{Fe2}}y}{k_{1\mathrm{Fe2}}}}, \qquad (1_1)$$

$$\frac{\mathrm{d}y}{\mathrm{d}t} = \frac{k_{0\mathrm{Fe2}}}{1+\dfrac{k_{0\mathrm{Fe2}}y}{k_{1\mathrm{Fe2}}}} + \frac{k_{0\mathrm{B3}}}{1+\dfrac{k_{0\mathrm{B3}}y}{k_{1\mathrm{B3}}}} \quad \frac{q}{sg} \quad \frac{k_{0B2}}{1+\dfrac{k_{0\mathrm{B2}}x}{k_{1\mathrm{B2}}}}, \qquad (1_2)$$

where x is the outer FeB layer thickness; y is the inner Fe_2B layer thickness; $k_{0\mathrm{Fe1}}$ and $k_{0\mathrm{B2}}$ are the chemical growth-rate constants of the FeB layer at the expense of diffusion of iron and boron atoms, respectively; $k_{1\mathrm{Fe1}}$ and $k_{1\mathrm{B2}}$ are the diffusional (physical) growth-rate constants of the FeB layer at the expense of diffusion of iron and boron atoms, respectively; $k_{0\mathrm{Fe2}}$ and $k_{0\mathrm{B3}}$ the chemical growth-rate constants of the Fe_2B layer at the expense of diffusion of iron and boron atoms, respectively; $k_{1\mathrm{Fe2}}$ and $k_{1\mathrm{B3}}$ are the diffusional (physical) growth-rate constants of the Fe_2B layer at the expense of diffusion of iron and boron atoms, respectively; g is the ratio of the molar volumes of the FeB and Fe_2B compounds; $p = q = r = 1$ and $s = 2$ (factors from the chemical formulae of FeB (written as BFe) and Fe_2B (BFe_2)).

The value of g is determined from the density of the compounds FeB (BFe) $_1$ = 6.70 10^3 kg m^{-3} and Fe_2B

(BFe_2) $_2$ = 7.34 10^3 kg m^{-3} [2] and their molecular mass M_1 = 66.65 g mol^{-1} and M_2 = 122.49 g mol^{-1}: g = $M_1\$_2/M_2$ $_1$ = 0.60.

From the system (1), it follows that initially growth kinetics of compound layers must be linear because at low t the terms of the type k_0x/k_1 and k_0y/k_1 can be neglected in comparison with unity. Therefore, this system takes the linear form

$$\frac{dx}{dt} = k_{0Fe1} + k_{0B2} \quad \frac{rg}{p} \; k_{0Fe2}, \qquad (2_1)$$

$$\frac{dy}{dt} = k_{0Fe2} + k_{0B3} \quad \frac{q}{sg} \; k_{0B2}. \qquad (2_1)$$

System of equations (2) describes the reaction controlled stage of growth of boride layers when the rates of diffusion of iron and boron atoms across layer bulks are very high and therefore their effect on the overall rates of formation of the layers is negligible in comparison with that of the rates of subsequent chemical transformations taking place at phase interfaces. Hence, purely chemical processes are rate-determining (chemical control), for there is a great excess of diffusing atoms of both kinds for both layers to grow. It does not mean, however, that the FeB and Fe_2B layers will necessarily occur and grow at the alloy (steel)-boron interface simultaneously.

Clearly, their simultaneous occurrence is only possible, if both derivatives dx/dt and dy/dt in equations (1) and (2) are positive, dx/dt > 0 and dy/dt > 0, and consequently the inequalities $k_{0Fe1} + k_{0B2} > (rg/p)k_{0Fe2}$ and $k_{0Fe2} + k_{0B3} > (q/sg)k_{0B2}$ are satisfied. In such a case, both boride layers will grow simultaneously from the very start of interaction of initial substances according to a linear law. It should be noted that the linear stage of growth of boride layers typical of thin films is not yet explored.

If the condition

$$k_{0Fe1} + k_{0B2} < \frac{rg}{p} \; k_{0Fe2} \qquad (3)$$

is satisfied, the FeB layer cannot form at all (dx/dt < 0). Therefore, only the Fe_2B layer is observed to grow at the alloy (steel)–boron interface. If the FeB layer were in an artificially prepared sample, its thickness would decrease, and it might eventually disappear completely, being kinetically (not thermodynamically) unstable.

From the system (1), it is seen that the sequential formation of boride layers (dx/dt < 0, dy/dt > 0 or dx/dt > 0, dy/dt < 0) is more probable than simultaneous (dx/dt > 0 and dy/dt > 0), the ratio of probability being 2 : 1. If their formation is not simultaneous, this system indicates a necessary condition for the occurrence of a next layer. As long as the Fe_2B layer is the first to occur, the FeB layer can only start to form when dx/dt > 0. Hence,

$$k_{0Fe1} + k_{0B2} \quad \frac{rg}{p} \; \frac{k_{0Fe2}}{1 + \frac{k_{0Fe2} y_{min}}{k_{1Fe2}}} \qquad (4)$$

where y_{min} is a smallest (minimal) thickness of the Fe_2B layer necessary for the FeB layer to occur and grow. Chemically, it merely means that at this thickness of the Fe_2B layer, the rate of consumption of the FeB layer during growth of the Fe_2B layer becomes first equal to and then less than the rate of its growth.

Growth kinetics of boride layers at the diffusional stage of their formation are described by a system of two differential equations

$$\frac{dx}{dt} = \frac{k_B}{x} \quad \frac{rg}{p} \; \frac{k_{Fe}}{y}, \qquad (5_1)$$

$$\frac{dy}{dt} = \frac{k_{Fe}}{y} \quad \frac{q}{sg} \; \frac{k_B}{x}, \qquad (5_2)$$

where x is the outer FeB layer thickness, y is the inner Fe_2B layer thickness, k_B is the FeB layer growth-rate constant, k_{Fe} is the Fe_2B layer growth-rate constant.

Calculations showed this system to provide a good fit to experimental data obtained with iron boride and other compound layers. Full set of appropriate values of diffusional constants k can be found in [40-49].

3.4. Microhardness and Abrasive Wear Resistance of Boride Layers

3.4.1. Microhardness of Boride Phases

With the alloys and steels investigated, numerical values of microhardness HV_{100} fall in the range 13-21 GPa for the FeB layer and 12-21 GPa for the Fe_2B one [49]. Microhardness varies considerably within both boride layers, especially those with the second type of microstructure in view of their non-homogeneity. The difference in microhardness of near-boride and far-away regions of the alloys or steels was insignificant (around 0.2 GPa).

The values obtained are close to those reported in the literature [1-7]. Somewhat higher values for Fe–25% Cr and Fe–30 % Cr alloys compared to Fe–5% Cr, Fe–10% Cr and Fe–15 % Cr ones are probably due to the difference in their microstructures, the two-phase microstructure being more rigid and therefore harder than the single-phase homogeneous one.

3.4.2. Dry Abrasive Wear Resistance of Boride Layers

Boriding the alloy and steel tablets for dry abrasive wear resistance tests were carried out at 950ºC for 21600 s (6 h). Wear resistance values are greater for the middle part of boride layers than for their borders with adjacent phases due to its more developed texture and more ordered microstructure.

Comparative data on the wear resistance of the outer boride layer for the alloys and steels investigated are provided in Table **5** [49]. Its values proved to increase disproportionately with increasing chromium content of the alloys and steels.

Borided materials with the layers of type I microstructure consisting of a homogeneous solid solution of chromium in the FeB compound or in the Fe_2B one exhibit a rather moderate increase in wear resistance compared to their bases. It is 5-15 times for a Fe–10% Cr alloy and 6-27 times for at 13% Cr steel.

A much greater increase is observed if the boride layers with a microstructure of type II are formed. For a Fe–25% Cr alloy it varies from 150 to 350 times. Boride layers with a microstructure of type II are so wear resistant that it is impossible to reach not only the alloy or steel base but even the inner layer by carrying out a reasonable number of tests. For this reason, comparison of the wear resistance values in Table **5** is restricted to the data for the outer boride layers.

In boride layers with type II microstructure, the (Cr,Fe)B phase (thin platelets, less than 100 nm thick) forms a rigid framework filled with the (Fe,Cr)B phase. Such network-platelet morphology results in enhanced wear resistance of the outer boride layer. The same applies to the inner boride layer consisting of $(Cr,Fe)_2B$ platelets embedded into the $(Fe,Cr)_2B$ matrix.

Thus, in order to increase the wear resistance of any product or part made of an ordinary iron-base alloy or steel, it is advisable first to cover its surface, for example galvanically, with a Fe–Cr alloy containing 25±5% chromium. Then, it is borided under carefully controlled temperature-time conditions based on the available kinetic data to ensure the necessary thickness and quality of a boride coating. If too high, brittleness of the coating obtained may be lowered by its alloying with Al, Si and other elements. Other thermochemical treatments may also be applied for this purpose.

4. CONCLUSIONS

Two boride layers occur in a coating on Fe–Cr alloys and chromium steels in the temperature range of 850–950ºC and reaction times up to 43200 s.

In the case of Fe–5% Cr, Fe–10% Cr and Fe–15% Cr alloys and a 13% Cr steel, the outer boride layer bordering the boriding agent consists of the (Fe,Cr)B

Table 5: Comparison of Wear Resistance Values of the Outer FeB Layer for the Fe–Cr Alloys and Chromium Steels [49]

Alloy or Steel	5% Cr Alloy	10% Cr Alloy	13% Cr Steel	15% Cr Alloy	25% Cr Steel	25% Cr Alloy	30% Cr Alloy
	Microstructure of Type I				Microstructure of Type II		
$\#m_{base}$ (g)	0.42335	0.32130	0.24335	0.31060	0.25730	0.29910	0.27740
$\#h_{base}$ (mm)	0.47	0.43	0.30	0.41	0.31	0.38	0.37
r_1	1	1.32	1.74	1.36	1.65	1.42	1.53
$\#m_{boride\ layer}$ (g)	0.03853	0.02875	0.02645	0.00695	0.00100	0.00095	0.00090
$\#h_{boride\ layer}$ (mm)	0.040	0.035	0.030	0.010	~.0.003	~0.003	~0.003
r_2	11.0	11.2	9.2	44.7	257.3	314.8	308.5
r_3	1	1.34	1.46	5.54	38.5	40.6	42.8

Note: $\#m$ and $\#h$ are changes in mass and height, respectively, of a sample;
$r_1 = \#m_{\text{base of a 5\% Cr alloy}} / \#m_{\text{base of a given material}}$;
$r_2 = \#m_{\text{base of a given material}} / \#m_{\text{boride layer on a given material}}$;
$r_3 = \#m_{\text{boride layer on a 5\% Cr alloy}} / \#m_{\text{boride layer on a given material}}$.

phase, whereas the inner boride layer adjacent to the solid substrate consists of the $(Fe,Cr)_2B$ phase. Each layer is a homogeneous phase (microstructure of type I).

Each of the layers formed on the surface of Fe–25% Cr and Fe–30% Cr alloys and a 25% Cr steel consists of two phases and has a regular network-platelet morphology (microstructure of type II).

Layer formation is sequential. The first layer to occur is $(Fe,Cr)_2B$.

Both boride layers possess a pronounced {002} texture. It causes their columnar microstructure.

Mechanism of formation of the layers generally includes the counter-diffusion of boron and iron (chromium) atoms across their bulks followed by subsequent chemical transformations at layer interfaces.

Boride layers with the microstructure of the second type exhibit a much higher wear resistance than those with the microstructure of the first type, the difference exceeding an order of magnitude.

ACKNOWLEDGMENTS

The author acknowledges with sincere gratitude waiving the publication cost by Synchro Publisher.

REFERENCES

[1] Glukhov VP. Boride coatings on iron and steels. Kiev: Naukova Dumka; 1970.

[2] Voroshnin LG, Lyakhovich LS. Boriding of steel. Moskwa: Metallurgiya; 1978.

[3] Matuschka AG. Boronizing. Munchen: Carl Hanser Verlag; 1980.

[4] Voroshnin LG. Boriding of industrial steels and cast irons. Minsk: Belarus; 1981.

[5] Sinha AK. Boriding (Boronizing). In: Sinha AK, ed. Metals Handbook. Metals Park, Ohio: ASM International; 1982.

[6] Kunst H, Haase B, Malloy J, Wittel K, Nestler MC, Nicoll AR, *et al*. Metals: surface treatment. In: Ullmann's encyclopedia of industrial chemistry. Weinheim: Viley–VCH; 2006.
http://dx.doi.org/10.1002/14356007.a16_403.pub2

[7] Holmberg K, Matthews A. Coatings tribology. Amsterdam: Elsevier; 2009.

[8] Hansen M. Constitution of binary alloys. 2nd ed. New-York: McGraw-Hill; 1958.

[9] Vol AE. Structure and properties of binary metallic systems, v.1. Moskwa: Fizmatgiz; 1962.

[10] Massalski TB, Murray JL, Bennett LH, Baker H. Binary alloy phase diagrams, v. 1. American Society of Metals, Metals Park, Ohio: ASM; 1986.

[11] Kuzma YB, Chaban NF. Binary and ternary systems containing boron. %oskwa: Metallurgiya; 1990.

[12] Okamoto H. B-Fe (Boron-iron). J Phase Equil Diff. 2004; 25: 297-298.
http://dx.doi.org/10.1007/s11669-004-0128-3

[13] Goeuriot P, Fillit R, Thevenot F, Driver JH, Bruyas H. The influence of alloying element additions on the boriding of steels. Mater Sci Eng. 1982; 55(1): 9-19.
http://dx.doi.org/10.1016/0025-5416(82)90078-7

[14] Carbucicchio M, Sambogna G. Influence of chromium on boride coatings produced on iron alloys. Thin Solid Films 1985; 126(3/4): 299-305.
http://dx.doi.org/10.1016/0040-6090(85)90324-4

[15] Brakman CM, Gommers AWJ, Mittemeijer EI. Boriding of Fe and Fe-C, Fe-Cr and Fe-Ni alloys: boride-layer growth kinetics. J Mater Res. 1989; 4(6): 1354-1370.
http://dx.doi.org/10.1557/JMR.1989.1354

[16] Fellner P, Chrenkova M. Rate of growth of boride layers on highly alloyed steels. Chem Papers 1992; 46(4): 226-231.

[17] Campos I, Oseguera J, Figueroa U, Garcia JA, Bautista O, Kelemenis G. Kinetic study of boron diffusion in the paste-boriding process. Mater Sci Eng A 2003; 352(1/2): 261-265.
http://dx.doi.org/10.1016/S0921-5093(02)00910-3

[18] Genel K, Ozbek I, Bindal C. Kinetics of boriding of AISI W1 steel. Mater Sci Eng A 2003; 347(1/2): 311-314.
http://dx.doi.org/10.1016/S0921-5093(02)00607-X

[19] Kulka M, Pertek P. Microstructure and properties of borided 41Cr4 steel after laser surface modification with re-melting. Appl Surf Sci. 2003; 214: 278-288.
http://dx.doi.org/10.1016/S0169-4332(03)00500-2

[20] Martini C, Palombarini G, Carbucicchio M. Mechanism of thermochemical growth of iron borides on iron. J Mater Sci. 2004; 39(3): 933-937.
http://dx.doi.org/10.1023/B:JMSC.0000012924.74578.87

[21] Taktak S. A study on the diffusion kinetics of borides on boronized Cr-based steels. J Mater Sci. 2006; 41(22): 7590-7596.
http://dx.doi.org/10.1007/s10853-006-0847-4

[22] Tian X, Lu Y, Sun SJ, Wang ZG, Hao WQ, Zhu XD, *et al*. Effect of boronising on mechanical properties, wear and corrosion of N80 steel. Mater Sci Techn. 2008; 24(3): 314-319.
http://dx.doi.org/10.1179/174328408X278448

[23] Oliveira CKN, Casteletti LC, Lombardi Neto A, Totten GE, Heck SC. Production and characterization of boride layers on AISI D2 tool steel. Vacuum 2010; 84(6): 792-796.
http://dx.doi.org/10.1016/j.vacuum.2009.10.038

[24] Campos-Silva I, Ortiz-Dominguez M, Lopez-Perrusquia N, Meneses-Amador A, Escobar-Galindo R, Martinez-Trinidad J, Characterization of AISI 4140 borided steels. Appl Surf Sci. 2010; 256(8): 2372-2379.
http://dx.doi.org/10.1016/j.apsusc.2009.10.070

[25] Jiang J, Wang Y, Zhong Q, Zhou Q, Zhang L. Preparation of Fe2B boride coating on low-carbon steel surfaces and its evaluation of hardness and corrosion resistance. Surf Coat Techn. 2011; 206(2-3): 473-478.
http://dx.doi.org/10.1016/j.surfcoat.2011.07.053

[26] Kiratli N, Findik F. Research on wear characteristics of AISI 1035 steel boronized at various parameters. Industr Lubr Tribol. 2011; 63(2): 127-133.
http://dx.doi.org/10.1108/00368791111116366

[27] Campos-Silva I. The boriding process: growth kinetics and mechanical characterization of boride layers. Jestech 2012; 15(2): 53-61.

[28] Gunes I. Kinetics of borided gear steels. Sadhana 2013; 38(3): 527-541.
http://dx.doi.org/10.1007/s12046-013-0138-0

[29] Sutrisno SB, Hikam M. Surface hardening of St41 low carbon steel by using the boronizing powder and pressured-heating technique. Res J Mater Sci. 2013; 1(10): 1-5.

[30] Joshi AA, Hosmani SS. Pack-boronizing of AISI 4140 steel: boronizing mechanism and the role of container design. Mater Manufact Process. 2014; 29: 1062-1072.

http://dx.doi.org/10.1080/10426914.2014.921705

[31] Zuno-Silva J, Ortiz-Dominguez M, Keddam M, Elias-Espinosa M, Damian-Mejia O, Cardoso-Legorreta E, *et al*. Boriding kinetics of Fe_2B layers formed on AISI 1045 steel. J Min Metall Sect B-Metall. 2014; 50(2): 101-107.

http://dx.doi.org/10.2298/JMMB140323019Z

[32] Dybkov VI. Reaction diffusion and solid state chemical kinetics. 2nd ed. Zuerich: Trans Tech Publications; 2010.

[33] Dybkov VI. Solid state reaction kinetics. Kyiv: IPMS Publications; 2013.

[34] Dybkov VI. Chemical Kinetics. Kyiv: IPMS Publications; 2013.

[35] Gurov KP, Kartashkin BA, Ugaste YE. Mutual diffusion in multiphase metallic systems. Moskwa: Nauka; 1981.

[36] Gusak AM, Zaporozhets TV, Lyashenko YO, Kornienko SV, Pasichnyy MO, Shirinyan AS. Diffusion-controlled solid state reactions: in alloys, thin-films and nanosystems. Berlin: Wiley-VCH; 2010.

http://dx.doi.org/10.1002/9783527631025

[37] Bondar AA. Boron-chromium-iron. In: Effenberg G, Ilyenko S, eds. Landolt-Bornstein 11D1. Berlin-Heidelberg: Springer; 2007. p. 320-343.

[38] Dybkov VI, Lengauer W, Barmak K. Formation of boride layers at the Fe–10%Cr alloy-boron interface. J Alloys Compd. 2005; 398(1/2): 113-122.

http://dx.doi.org/10.1016/j.jallcom.2005.02.033

[39] Dybkov VI. Diffusional growth kinetics of boride layers at the 13% Cr steel interface with amorphous boron. Defect Diffusion Forum 2007; 263: 183-188.

http://dx.doi.org/10.4028/www.scientific.net/ddf.263.183

[40] Dybkov VI. Growth of boride layers on the 13% Cr steel surface in a mixture of amorphous boron and KBF_4. J Mater Sci. 2007; 42(16): 6614-6627.

http://dx.doi.org/10.1007/s10853-007-1512-2

[41] Dybkov VI, Goncharuk LV, Khoruzha VG, Meleshevich KA, Samelyuk AV, Sidorko VR. Diffusional growth kinetics of boride layers on iron-chromium alloys. Solid State Phenomena 2008; 138: 181-187.

http://dx.doi.org/10.4028/www.scientific.net/SSP.138.181

[42] Dybkov VI, Sidorko VR, Khoruzha VG, Samelyuk AV, Goncharuk LV. Interaction of 25% chromium steel with boron powder. Poroshkovaya Metallurgiya 2011; (7/8): 222-230.

[43] Dybkov VI, Goncharuk LV, Khoruzha VG, Samelyuk AV, Sidorko VR. Growth kinetics and abrasive wear resistance of boride layers on Fe–15% Cr alloy. Mater Sci Technol. 2011; 27(10): 1502-1512.

http://dx.doi.org/10.1179/026708310X12683157551577

[44] Dybkov VI, Sidorko VR, Goncharuk LV, Khoruzha VG, Samelyuk AV. Microstructure, growth kinetics and abrasive wear resistance of boride layers on Fe–30% Cr alloy. Poroshkovaya Metallurgiya 2012; (9/10): 24-37.

[45] Dybkov VI. Effect of microstructure on the wear resistance of borided Fe–Cr alloys. Intern J Mater Res. 2013; 104(7): 617-629.

http://dx.doi.org/10.3139/146.110915

[46] Dybkov VI. Boride coatings of Fe–Cr alloys and chromium steels. Intern J Mater Chem Phys. 2015; 1(1): 43-66.

[47] Dybkov VI. Thermochemical boriding of iron–chromium alloys. Chemistry J. 2015; 1(3): 81-89.

[48] Dybkov VI. Thermochemical boriding of Fe–5% Cr alloy. Poroshkovaya Metallurgiya 2015; (11/12): 27-42.

[49] Dybkov VI. Thermochemical boriding of iron-chromium alloys. Kyiv: IPMS Publications; 2015.

[50] Mirkin LI. Handbook on x-ray analysis of polycrystals. Moskwa: Fizmatgiz; 1961.

[51] Gorelik SS, Rastorguev LN, Skakov YA. X-ray and electron-optical analysis: appendixes. Moskwa: Metallurgiya; 1970.

[52] Barinov VA, Dorofeev GA, Ovechkin LV, Elsukov EP, Ermakov AE. Structure and magnetic properties of the !-FeB phase obtained by mechanical working. Phys Stat Solidi A 1991; 123: 527-534.

http://dx.doi.org/10.1002/pssa.2211230217

[53] Gianoglio C, Badini C. Distribution equilibria of iron and nickel in two phase fields of the Fe-Ni-B system. J Mater Sci. 1986; 21: 4331-4334.

http://dx.doi.org/10.1007/BF01106551

[54] Okada S, Atoda T, Higashi I. Structural investigation of Cr_2B_3, Cr_3B_4, and CrB by single-crystal diffractometry. J Sol St Chem. 1987; 68: 61-67.

http://dx.doi.org/10.1016/0022-4596(87)90285-4

[55] Gianoglio C, Pradelli G, Vallino M. Solid state equilibria in the Cr-Fe-B system at the temperature of 1373 K. Metallurg Sci Techn. 1983; 1: 51-57.

[56] Keddam M. A kinetic model for the borided layers by the paste-boriding process. Appl Surf Sci. 2004; 236(1): 451-455.

http://dx.doi.org/10.1016/j.apsusc.2004.05.141

[57] Keddam M. Simulation of the growth kinetics of FeB and Fe2B phases on the AISI M2 borided steel: Effect of the paste thickness. Intern J Mater Res. 2009; 100(6): 901-905.

http://dx.doi.org/10.3139/146.110125

Received on 08-03-2016 Accepted on 14-03-2016 Published on 25-03-2016